A generalized boundary condition for generating wave–current coupling flows in a 3D numerical tank

Hong-Guan Lyu, Peng-Nan Sun*
School of Ocean Engineering and Technology
Sun Yat-sen University
Zhuhai 519082, China
lyuhg@mail.sysu.edu.cn; sunpn@mail.sysu.edu.cn

I. Introduction

As one of the most popular meshless CFD methods, SPH has received much attention in coastal and ocean engineering community due to its capability of handling violent free-surface flows involving breaking and splashing. Nevertheless, in most SPH literature, a wave field has been generated usually by employing a movable wave paddle with a prescribed motion signal. Despite the fact that such a strategy is easy-to-implement in coding and matches perfectly the Lagrangian nature of SPH, it is hard to produce current-alone or wave-current coupling fields that are also quite important in marine hydrodynamics simulations. One may found that this issue has received rather limited attention from the SPH community in the past [1]. There were some research works attempting to generate a current-alone field by different strategies (e.g. [2]), while generating a wave-current coupling field has been still a challenging task.

In this paper, a generalized boundary condition is presented to generate wave-alone, current-alone, and wave–current coupling fields. The main characteristics of the present boundary condition can be attributed to two points. First of all, it exploit the technique called Lagrangian particle injector that generates and removes a fluid particle based on the principle of mass flux conservation, by converting Eulerian flow information into Lagrangian ones on a specific plane. Secondly, it is able to generate a desired ocean field not only by imposing a Dirichlet source boundary but also by coupling with an external CFD solver; the latter means that by enforcing the present boundary condition, one can leverage the respective advantages of different CFD methods to perform a marine hydrodynamics simulation involving wave or current generation.

II. Numerical scheme

The overall configuration of the present numerical tank in 3D and 2D views are illustrated in Figures 1(a) and 1(b), respectively. As one can see, the present numerical tank is divided into three regions, i.e. upstream, midstream, and downstream regions. A series of particles with a rectangular and single-layer layout is distributed at the source boundary of the numerical tank; hereinafter, these particles are referred to as injector particles. The particle size Δr of an injector particle is adopted as the reference size of the simulation. More importantly, an exclusive

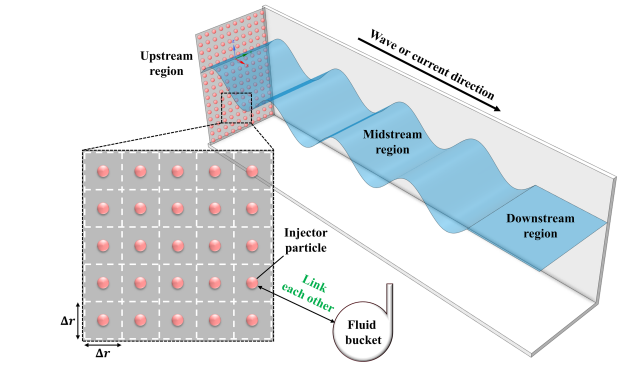

(a) 3D view with the principle of Lagrangian particle injector

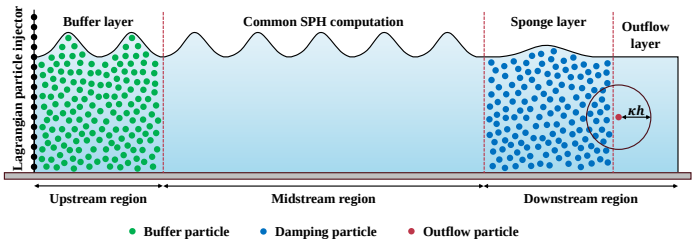

(b) 2D view with the decomposition of the computational region

Fig. 1. Overall configuration of the present numerical tank

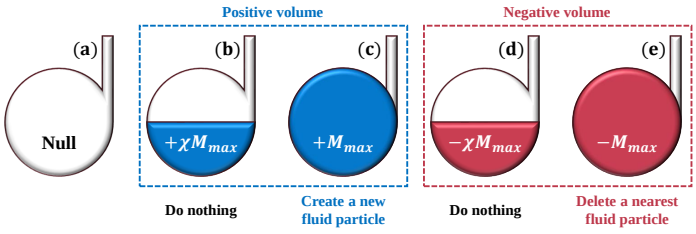

Fig. 2. Five possible phases of a fluid bucket during a simulation

fluid bucket is assigned to each injector particle, and both of them link to each other. Each fluid bucket is initialized to null at the beginning (see also panel (a) of Figure 2) and can be filled with a certain amount of fluid according to the local mass flux across the injector boundary. Note that the maximum filling mass of a fluid bucket is defined as $M_{max} = (\Delta r)^d$ where d

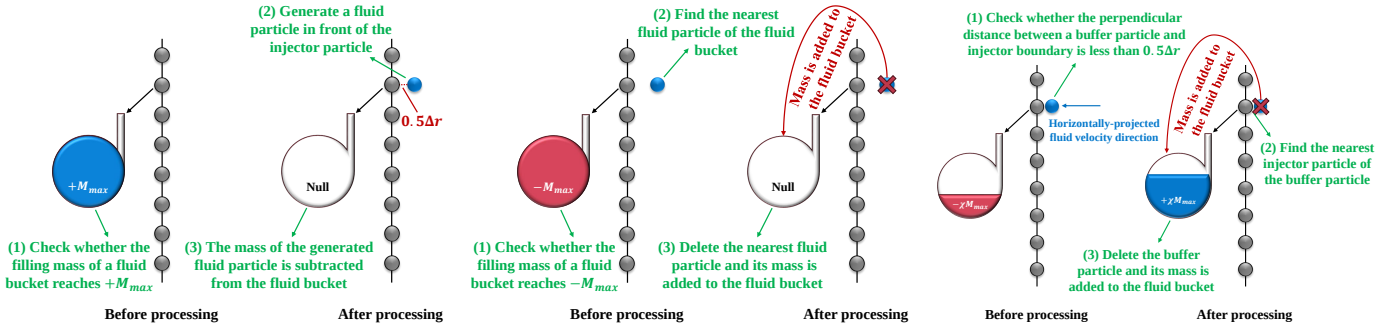

(a) Particle generating (b) Particle deleting (c) Particle leaving

Fig. 3. Processing principles when dealing with particle generating, deleting and leaving.

refers to the dimension of the simulation.

Once the spatiotemporal flow information on the injector boundary is known (this can be obtained by either enforcing Dirichlet source condition [3] or extrapolating from an external CFD solver [4]), the detailed procedure to generate a desired ocean field can be executed successively as follows:

- *Step 1: Calculating the filling mass of each fluid bucket via the local net mass transfer across the injector boundary*

At every time step, the local net mass transfer across the injector boundary at the location of the jth injector particle is computed. The net mass computed is then added to the fluid bucket associated with the jth injector particle, and the real-time filling mass of the jth fluid bucket at the kth time step, $M_j^{(k)}$, is evaluated by

$$M_j^{(k)} = M_j^{(k-1)} + \rho_0 \left(\Delta r\right)^{d-1} \left[\mathbf{v}_j^{(k)} \cdot \mathbf{n}\right] \Delta t^{(k)}, \qquad (1)$$

where $(\cdot)^k$ and $(\cdot)^{k-1}$ refer to a quantity at the kth and $(k-1)$th time step, respectively. ρ_0 refers to the reference density of the fluid. Δr denotes to the reference particle size. Δt represents the size of time step. $\mathbf{n}$ refers to the normal of the injector boundary (pointing positively to the inner of the numerical tank). $\mathbf{v}_j$ stands for the velocity at the location of the jth injector particle.

- *Step 2: Generating or deleting a fluid particle according to the filling mass of each fluid bucket*

After successfully executing the first step, there are four possible phases in a fluid bucket as shown in panels (b) - (e) of Figure 2. When the filling mass of the jth fluid bucket reaches $+M_{max}$, a fluid particle will be generated in front of the normal direction of the injector boundary with a perpendicular distance of $0.5\Delta r$. Meanwhile, the value of M_{max} is subtracted from the jth fluid bucket to maintain the local mass conservation (see Figure 3(a)). On the contrary, when the filling mass of the jth fluid bucket reaches $-M_{max}$, the fluid particle closest to the jth injector particle is deleted with its mass being added to the jth fluid bucket (see Figure 3(b)).

- *Step 3: Imposing analytically a velocity to each buffer particle and then updating their positions.*

As one can see in Figure 1(b), a buffer layer (hereinafter denoted by $\mathcal{B}$) is implemented in the upstream region to guarantee a smooth transition from the injector boundary (theoretical or extrapolated solutions) to the midstream region (SPH simulations). When the second step is executed successfully, the buffer layer, $\mathcal{B}$, is identified according to the following criteria:

$$\begin{cases} \|l_i\| \leq \sigma_b \Delta r, \ i \in \mathcal{B}, \\ \|l_i\| > \sigma_b \Delta r, \ i \notin \mathcal{B}, \end{cases} \quad \text{with} \quad l_i = \frac{\left(\mathbf{r}_i - \mathbf{r}_p\right) \cdot \mathbf{n}}{\|\mathbf{n}\|}, \qquad (2)$$

where l_i represents the perpendicular distance between the ith candidate particle and the injector boundary. $\mathbf{r}_p$ refers to a point distributed arbitrarily in the injector boundary. σ_b denotes a width coefficient of the buffer layer and is adopted as 10 in the present study.

Subsequently, the fluid velocity of each buffer particle is imposed directly from the ocean field of interest. After which, the position of each buffer particle is updated by the forward Euler's method.

- *Step 4: Removing each buffer particle that is about to leave the injector boundary and then updating again the filling mass of the fluid bucket nearest the removed buffer particle.*

It should be underlined that, for many common gravity waves in coastal and ocean engineering, the orbit of a fluid element could behave as a periodical oscillation around its balanced position, which means that a buffer particle is possible to cross the injector boundary during a simulation (i.e. leaving from the buffer layer to outside). When this occurs, special treatments are needed to maintain the flow consistency during the simulation. As illustrated in Figure 3(c), when the perpendicular distance between a buffer particle and the injector boundary is less than $0.5\Delta r$ and the fluid velocity of the buffer particle is opposite to the normal of the injector boundary, the buffer particle is regarded as the one that is about to cross the injector boundary. In this regime, the buffer particle is deleted directly and its mass is added to the fluid bucket nearest the buffer particle deleted. As a consequence, the exact filling mass of the jth fluid bucket is written as

$$M_j^{(k)} = M_{j,\ \text{Step1}}^{(k)} - M_{max} \mathbb{1}_{j \in \mathbb{S}_f} + \sum M_{max} \mathbb{1}_{j \in \mathbb{S}_p}, \qquad (3)$$

where $\mathbb{S}_f$ refers to the set of those fluid buckets that have generated particles in the second step, while $\mathbb{S}_p$ denotes the set of those fluid buckets that have received mass in either the second or fourth steps. $\mathbb{1}_{j\in(\cdot)}$ is an indicator function defined as

$$\mathbb{1}_{j\in(\cdot)} = \begin{cases} 1, & j \in (\cdot)\,, \\ 0, & j \notin (\cdot)\,. \end{cases} \tag{4}$$

Although the above procedure is introduced in a 3D scenario, it can be transformed into a 2D scenario without any difficulties. In that case, the injector boundary reduces from a 2D plane to a 1D line. Finally, we underlined again that the above procedure is not only suitable for wave-making and current-making but also for generating a wave-current coupling field as long as the flow information of the desired field is already known.

III. Benchmarks

Tow benchmarks are provided in this section. The first benchmark is to simulate a current interacting with a cylinder, in which the desired field is generated directly by a given current profile at the source boundary. As shown in Figure 4, the free-surface shape simulated by the present SPH-based numerical tank is in good agreement with the experimental snapshot. It is clear that the present numerical tank is capable of generating a desired current field by directly imposing an analytical boundary condition.

The second benchmark is to simulate a wave interacting with a vessel and the targeted field is produced by coupling with an external CFD solver named HOS-NWT, an open-source High Order Spectra (HOS) solver developed by LHEEA Laboratory in Centrale Nantes. The final numerical results are shown in Figure 5. The top panel shows the snapshot of the wave field when the crest passing through the vessel and the bottom panel displays the comparison of the pitching motion between SPH-HOS and ANSYS AQWA. As one can see, the present numerical tank is able to generate a desired wave field by coupling with an external CFD solver and satisfactory numerical results are obtained. From these two benchmarks, it is demonstrated that the present numerical tank possesses sufficient accuracy and stability in solving marine hydrodynamics problems.

IV. Conclusion

In this paper, a generalized boundary condition is presented for generating wave-alone, current-alone, and wave–current fields in a 3D numerical tank. The feasibility and reliability of the present numerical tank are demonstrated by two fully 3D benchmarks. It is shown that the present boundary condition is able to produce a desired ocean field in a simple manner by either imposing a Dirichlet source boundary or coupling with an external CFD solver, showing great potential to be applied in solving fully 3D coastal and ocean engineering problems involving wave or current generation.

Acknowledgment

This research is supported by the China Postdoctoral Science Foundation (Grant No. 2024M763748) and the National Natural Science Foundation of China (Grant No. 52171329).

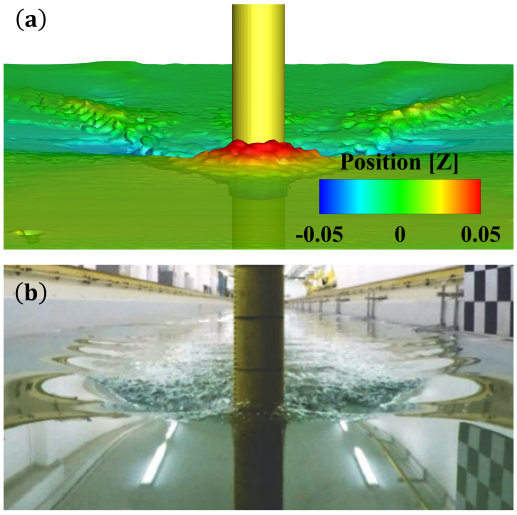

Fig. 4. Benchmark #1: Current interacting with a cylinder

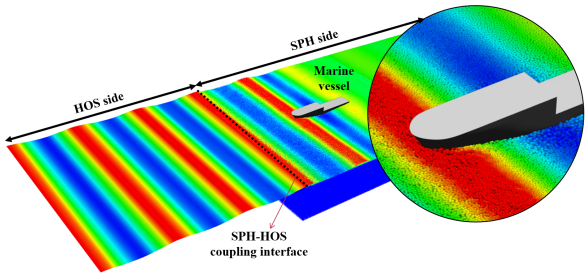

(a) Wave field when the crest passing through the vessel ($t = 80\,\mathrm{s}$)

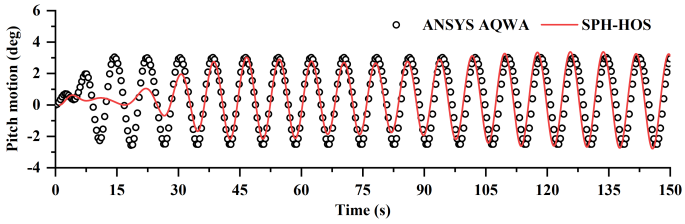

(b) Comparion of the pitching motion between SPH-HOS and ANSYS AQWA

Fig. 5. Benchmark #2: Wave interacting with a vessel

References

[1] Y. Yang, S. Draycott, P. K. Stansby, and B. D. Rogers, "A numerical flume for waves on variable sheared currents using smoothed particle hydrodynamics (sph) with open boundaries," Applied Ocean Research, vol. 135, p. 103527, 2023.

[2] A. Tafuni, J. Domínguez, R. Vacondio, and A. Crespo, "A versatile algorithm for the treatment of open boundary conditions in smoothed particle hydrodynamics gpu models," Computer methods in applied mechanics and engineering, vol. 342, pp. 604–624, 2018.

[3] H.-G. Lyu and P.-N. Sun, "Establishment and validation of a versatile sph-based numerical tank for generating wave-alone, current-alone, and wave-current-combined fields," Coastal Engineering, vol. 197, p. 104663, 2025.

[4] H.-G. Lyu, P.-N. Sun, J.-C. Yang, P.-Z. Liu, C.-M. Xie, and Y.-L. Ye, "Establishment and validation of a viscous-potential coupled and graphics processing unit accelerated numerical tank based on smoothed particle hydrodynamics and high-order spectral methods," Physics of Fluids, vol. 35, no. 10, 2023.